

## Supporting Information

### **Revitalizing inert carbon pores with benzoquinone for high-performance flexible zinc-ion capacitors**

Lintong Hu,<sup>†</sup> Xiaolong Li,<sup>†</sup> Yunpeng Zhou, Can Cui, Minjie Shi and Chao Yan\*

School of Materials Science and Engineering, Jiangsu University of Science and Technology, Zhenjiang, 212003, P. R. China.

<sup>†</sup> These authors contributed equally to this work.

\*Corresponding Author: chaoyan@just.edu.cn

## 1. Experimental Procedures

**Carbon electrode fabrication.** 40 mg Activated carbon (AC, YP-80, Kuraray,) was blended with 7.5 mg acetylene black using 2.5 mg polytetrafluoroethylene as a binder. The resulting mixture was then formed into a film and dried 12 h at 60 °C. The film has a mass loading of 3-4 mg cm<sup>-2</sup> and an average thickness of 135 μm. To prepare the AC electrode, the film (0.5 cm × 0.5 cm) was pressed onto a titanium mesh current collector.

**Electrolyte preparation.** ZnSO<sub>4</sub> was dissolved in deionized water to prepare a 2 M ZnSO<sub>4</sub> electrolytes. The zinc sulfate electrolyte containing BQ was made by dissolving a measured amount of BQ into the ZnSO<sub>4</sub> solution. All electrolytes are prepared before the experiment. The conductivity of the electrolyte is tested using a conductivity meter (DDSJ-307F, INESA). The ionic conductivity of 2 M ZnSO<sub>4</sub> electrolyte is 53 mS cm<sup>-1</sup>. After adding 30 mM BQ, the ionic conductivity is 54.4 mS cm<sup>-1</sup>. It indicates that the addition of BQ has a minimal impact on the conductivity of the ZnSO<sub>4</sub> electrolyte.

**Study of Electrolyte Stability.** A three-electrode system was used to study the cycling stability of BQ molecules. Zinc metal served as the reference electrode, a graphite rod as the counter electrode, and AC as the working electrode. The electrolyte consisted of 10 mM BQ + 2 M ZnSO<sub>4</sub>. Three samples were GCD cycled for 500, 1000, and 1500 cycles at a current density of 20 A g<sup>-1</sup>, after which the electrolyte was sampled and characterized using UV-vis spectroscopy.

**Gel electrolyte preparation.** The preparation method for the zinc ion gel electrolyte is illustrated in Fig. S1. First, 2.0 g acrylamide (AM) and the crosslinking

agent 1.4 mg N, N'-methylenebisacrylamide (MBA) are added sequentially to a 6 mL 2 M ZnSO<sub>4</sub> solution, followed by stirring and ultrasonic treatment 5 min to obtain Solution 1. Next, an initiator, 9.6 mg ammonium persulfate (APS), is added to 3 mL 2 M ZnSO<sub>4</sub> solution. Stir and ultrasonic treatment 5 min to obtain solution 2. After preparing both solutions, solution 2 is poured into solution 1, and the combined mixture is stirred to achieve a uniform precursor mixture. Finally, the mixture is stirred thoroughly once more before being transferred into a polytetrafluoroethylene (PTFE) mold (diameter: 10 cm, depth: 2 mm), and then placed in an oven at 80 °C for 10 minutes.

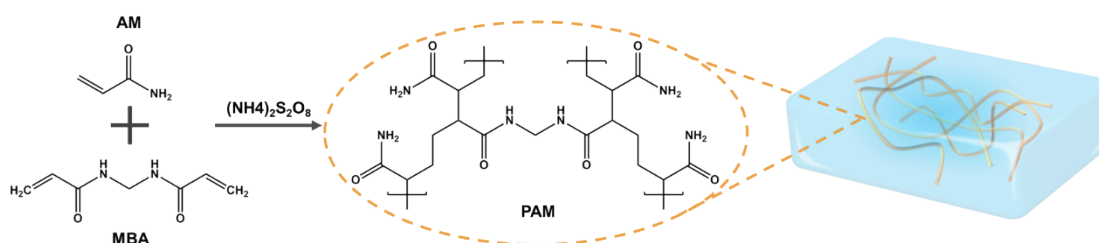


Fig. S1. The synthesis process of gel electrolyte.

**Electrochemical measurements of AC.** Regardless of the electrolyte used, the electrochemical performance of AC is tested using a three-electrode system, with a metal zinc foil serving as the reference and counter electrodes. The size of AC film is 0.5 cm × 0.5 cm with Ti mesh as the current collector.

**Capacitor device assembly process.** Zinc foil (thickness: 100 μm, size: 1 cm × 3 cm) is used as the anode, AC (3.5 mg cm<sup>-2</sup>, thickness: 135 μm) as the cathodes, and gel electrolyte (thickness: 3 mm, size: 1.5 cm × 3.5 cm) as the separator in the capacitors. Before assembly, the AC electrode (1.2 mg) is soaked in an electrolyte (2 M ZnSO<sub>4</sub> aqueous solution with 30 mM BQ, 1 mL) for 24 hours. The size of devices for

electrochemical and bending tests is  $1.5\text{ cm} \times 3.5\text{ cm}$ . The size of devices for powering a timer is  $4\text{ cm} \times 4\text{ cm}$ .

**Material characterization.** Scanning electron microscopy (SEM, Nova NanoSem450, FEI). Raman (LabRAM HR800, 532 nm laser). Nitrogen sorption analysis (Autosorb iQ Station). UV-vis spectroscope (UV2000).

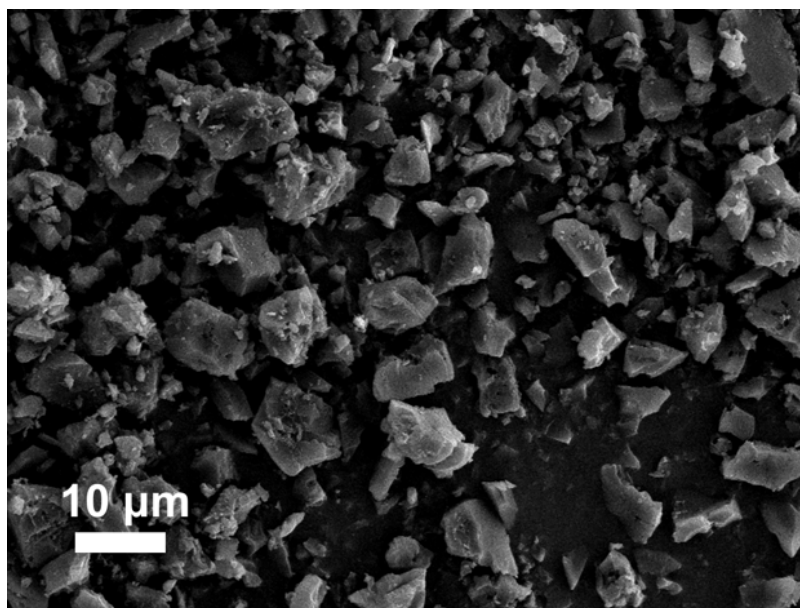


Figure S2. SEM image of the activated carbon.

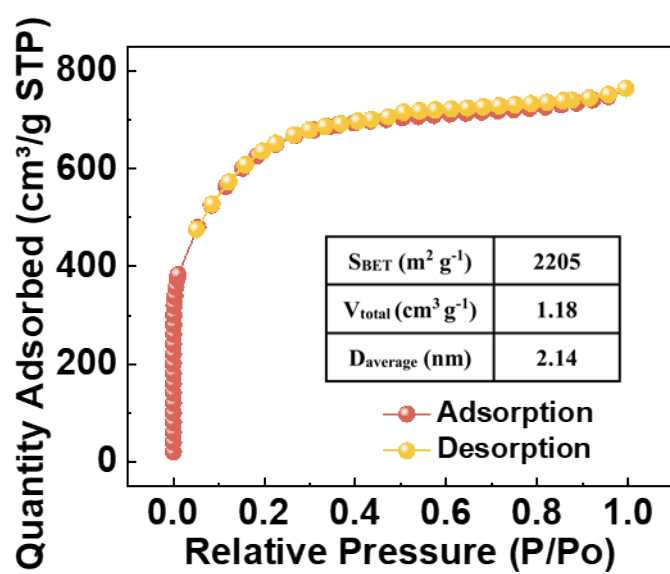


Figure S3. Nitrogen adsorption isotherm of the activated carbon.

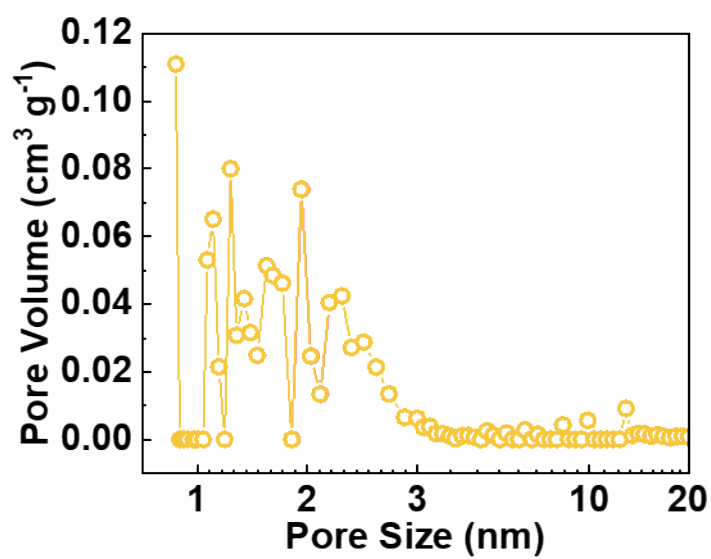


Figure S4. Pore size distribution of the activated carbon.

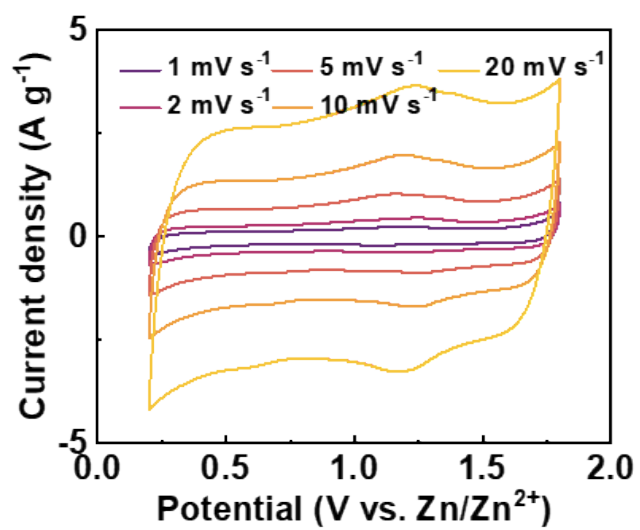


Figure S5. CV curves of AC in 2 M ZnSO<sub>4</sub> electrolyte.

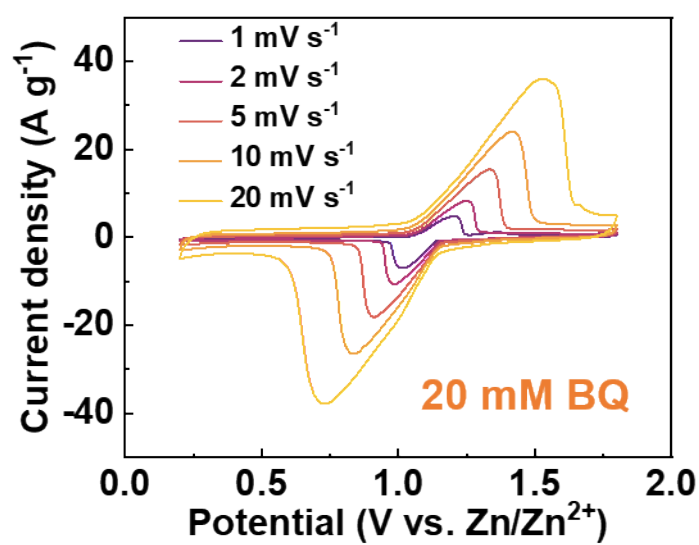


Figure S6. CV curves of AC in 2 M ZnSO<sub>4</sub> electrolyte with 20 mM BQ.

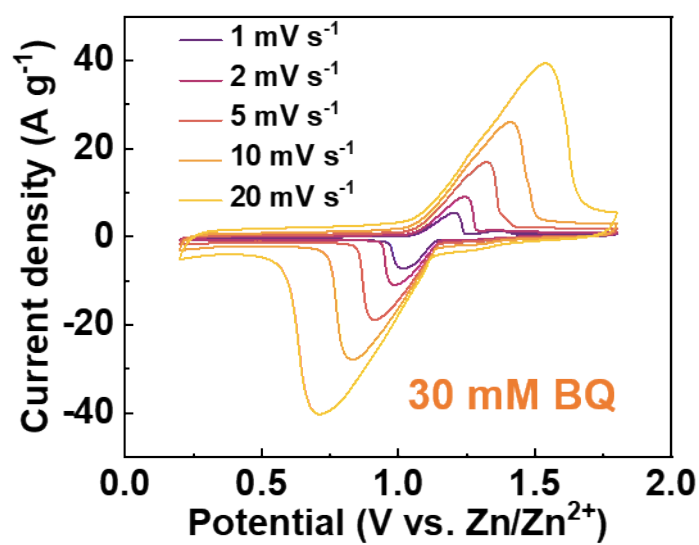


Figure S7. CV curves of AC in 2 M ZnSO<sub>4</sub> electrolyte with 30 mM BQ.

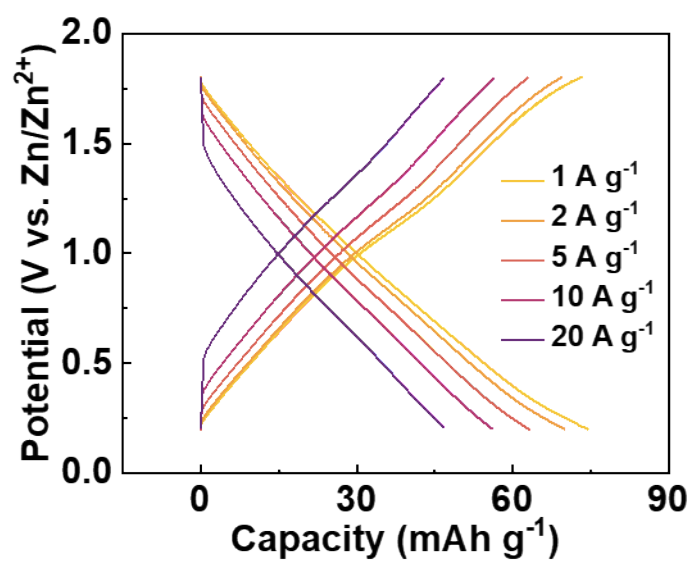


Figure S8. GCD curves of AC in 2 M ZnSO<sub>4</sub> electrolyte.

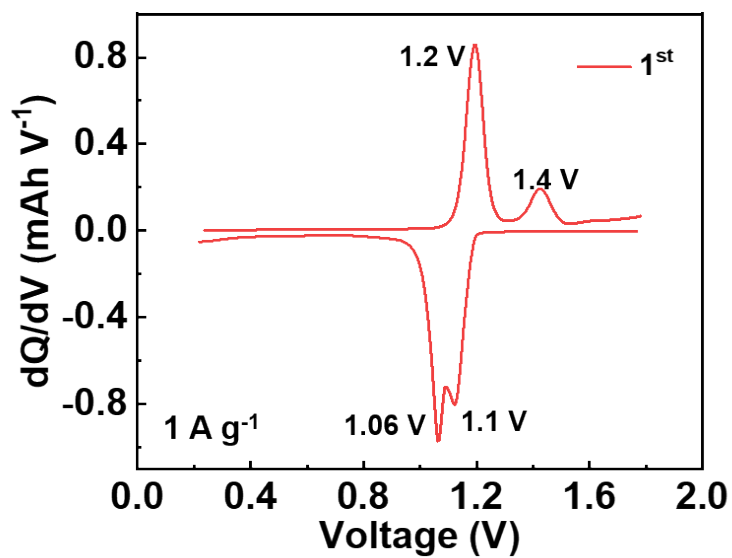


Figure S9. dQ/dV curve at the 1<sup>st</sup> cycle.



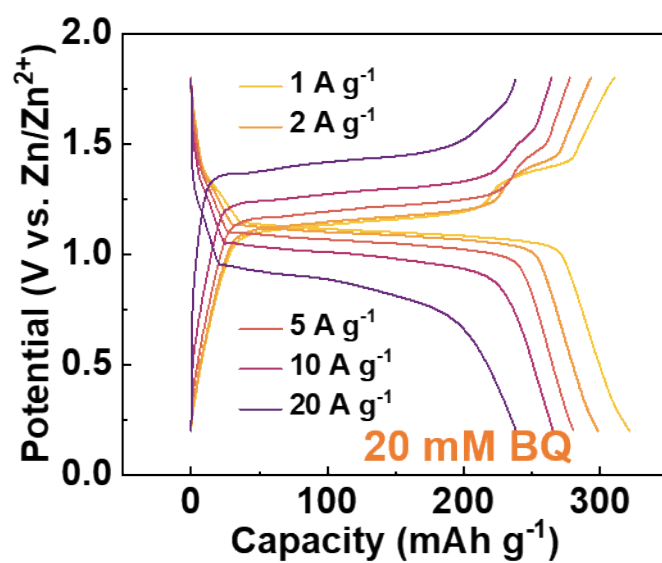


Figure S10. GCD curves of AC in 2 M ZnSO<sub>4</sub> electrolyte with 20 mM BQ.

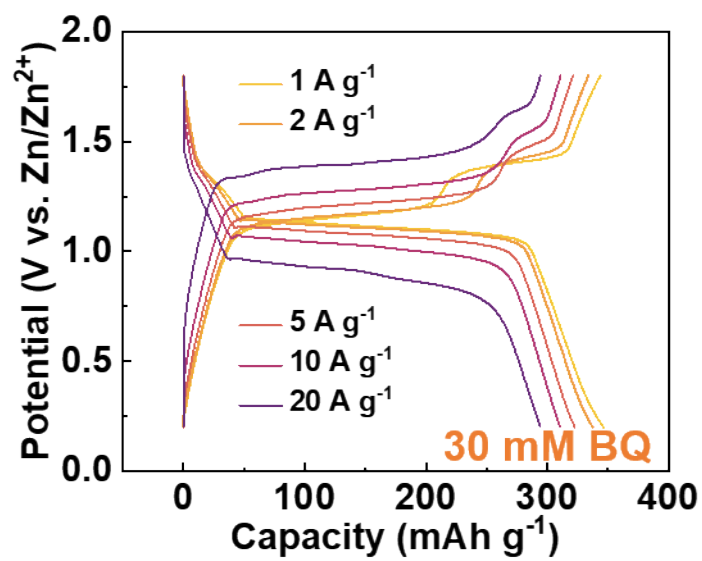


Figure S11. GCD curves of AC in 2 M ZnSO<sub>4</sub> electrolyte with 30 mM BQ.

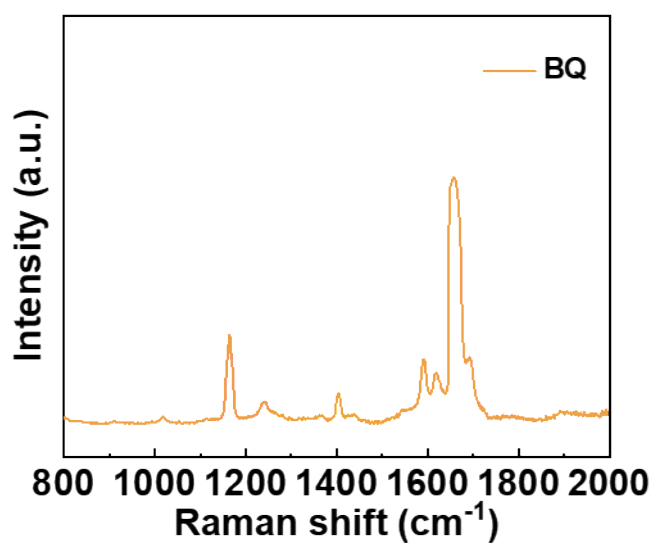


Figure S12. Raman spectrum of BQ powder. 1658  $\text{cm}^{-1}$  (C=O, C=C stretching vibration), 1618  $\text{cm}^{-1}$  (C=O, C=C stretching vibration), 1590  $\text{cm}^{-1}$  (C=C stretching vibration), 1400  $\text{cm}^{-1}$  (C-H deformation vibration), 1164  $\text{cm}^{-1}$  (C-H bending vibration).

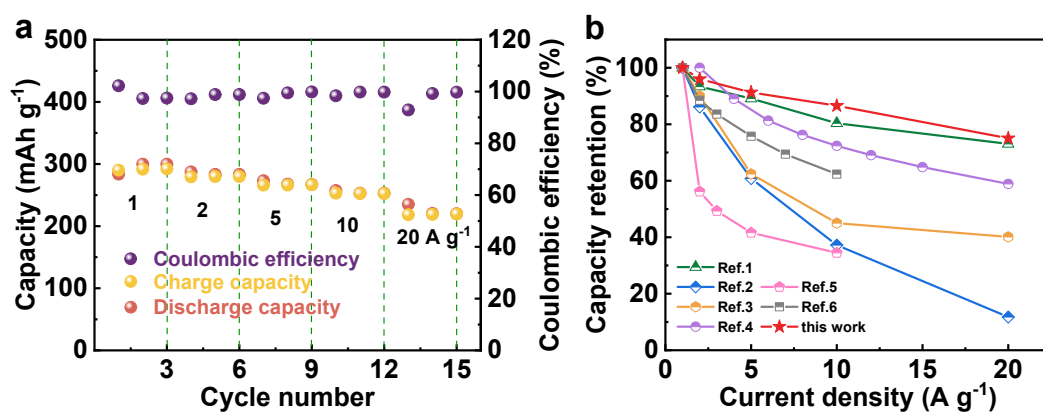


Figure S13. (a) Rate performance of the capacitors. (b) Performance comparison.

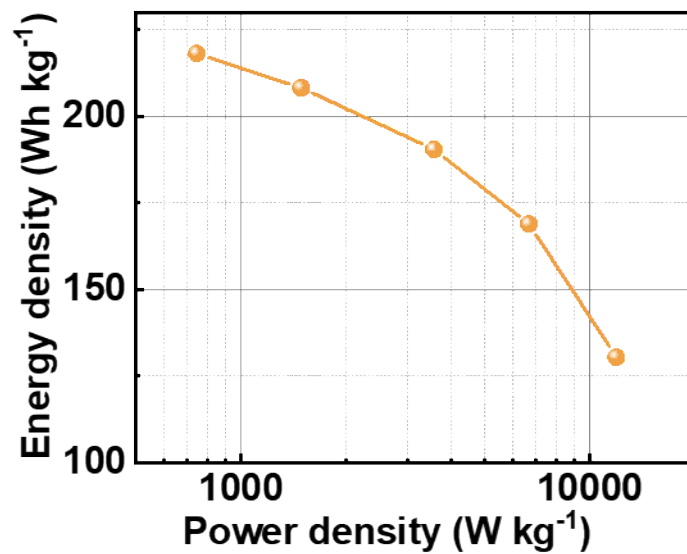


Figure S14. Ragone plot of the capacitors.

Table S1. Comparison of the energy density of zinc-ion capacitors.

Electrode material	Electrolyte	Energy density ( Wh kg <sup>-1</sup> )	Refs.
AC//Zn	PSBMA	110	7
MMSC-A//Zn	2 M ZnSO <sub>4</sub>	200	8
AC//AC	PAM/LA/PSBMA	110	9
AC//Zn	TC-7.5/PSA	80.5	10
AC//2D-Zn	2 M ZnSO <sub>4</sub>	208	11
CNTs//Zn	hydrogel electrolyte	104	12
C//Zn	CP/EGZn/betaine	142.8	13
AC//Zn	BQ/PAM	218	This work

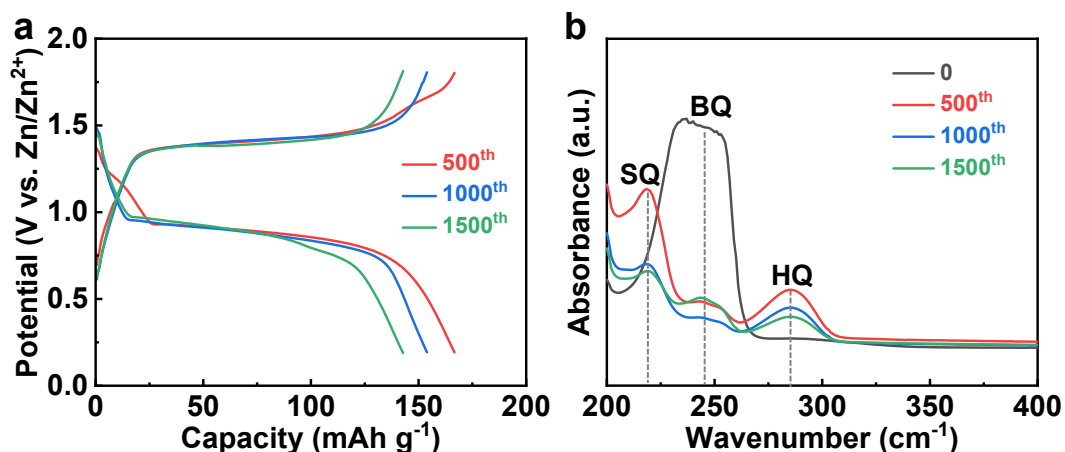


Figure S15. (a) GCD curves at 500<sup>th</sup>, 1000<sup>th</sup>, and 1500<sup>th</sup> cycles. (b) UV-vis spectrum of the electrolytes after 500<sup>th</sup>, 1000<sup>th</sup>, and 1500<sup>th</sup> cycles. The GCD plateaus potentials for the 500<sup>th</sup>, 1000<sup>th</sup>, and 1500<sup>th</sup> cycles are the same, but the capacities gradually decrease. Before cycles, the spectrum of the fresh electrolyte (10 mM BQ + 2 M ZnSO<sub>4</sub>) has a wide peak centered at 245 nm, which should be assigned to the BQ.<sup>14</sup> The spectra of the electrolyte after 500<sup>th</sup>, 1000<sup>th</sup>, and 1500<sup>th</sup> cycles show additional peaks at 219 nm and 285 nm, which may be related to semiquinone (SQ) and hydroquinone (HQ). The results indicate that there are three active substances in the electrolyte after a long period of cycling.

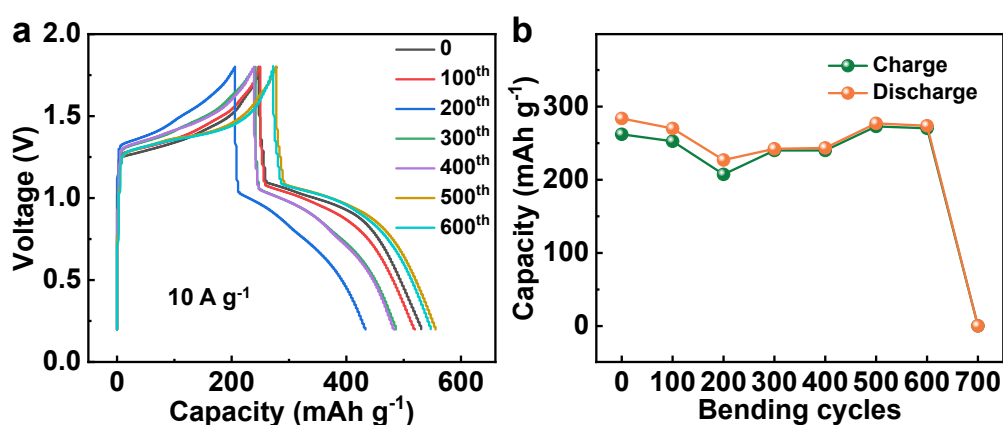


Figure S16. (a) GCD curves of the derives after different bending cycles, and (b) the corresponding charge and discharge capacity. The GCD curves exhibit distinct charge and discharge plateaus. The device capacity shows slight fluctuations. After 700 bending cycles, the device is fractured.

## References

1. K. Xiao, X. Jiang, S. Zeng, J. Chen, T. Hu, K. Yuan and Y. Chen, *Adv. Funct. Mater.*, 2024, **34**, 2405830.
2. X. Li, C. Cai, P. Hu, B. Zhang, P. Wu, H. Fan, Z. Chen, L. Zhou, L. Mai and H. J. Fan, *Adv. Mater.*, 2024, **36**, 2400184.
3. G.-H. An, J. Hong, S. Pak, Y. Cho, S. Lee, B. Hou and S. Cha, *Adv. Energy. Mater.*, 2020, **10**, 1902981.
4. C. Fang, B. Xu, J. Han, X. Liu, Y. Gao and J. Huang, *Adv. Funct. Mater.*, 2024, **34**, 2310909.
5. L. Wan, H. Zhang, M. Qu, M. Feng, Z. Shang, R. Wang, D. Lei and Y. Cui, *Energy. Storage. Mater.*, 2023, **63**, 102982.
6. Y.-G. Lee, G. Yoo, Y.-R. Jo, H.-R. An, B.-R. Koo and G.-H. An, *Adv. Energy. Mater.*, 2023, **13**, 2300630.
7. J. Zeng, H. Chen, L. Dong and X. Guo, *Adv. Funct. Mater.*, 2024, **34**, 2314651.
8. X. Li, C. Cai, P. Hu, B. Zhang, P. Wu, H. Fan, Z. Chen, L. Zhou, L. Mai and H. J. Fan, *Adv. Mater.*, 2024, **36**, 2400184.
9. S. Cui, W. Miao, X. Wang, K. Sun, H. Peng and G. Ma, *ACS Nano*, 2024, **18**, 12355-12366.
10. Q. Fu, S. Hao, L. Meng, F. Xu and J. Yang, *ACS Nano*, 2021, **15**, 18469-18482.
11. G. H. An, J. Hong, S. Pak, Y. Cho, S. Lee, B. Hou and S. Cha, *Adv. Energy. Mater.*, 2019, **10**, 1902981.
12. J. Nan, Y. Sun, F. Yang, Y. Zhang, Y. Li, Z. Wang, C. Wang, D. Wang, F. Chu, C. Wang, T. Zhu and J. Jiang, *Nano-Micro Lett.*, 2023, **16**, 22.
13. Q. Fu, S. Hao, X. Zhang, H. Zhao, F. Xu and J. Yang, *Energy Environ. Sci.*, 2023, **16**, 1291-1311.
14. Sirajuddin, M. Iqbal Bhangar, A. Niaz, A. Shah, A. Rauf, *Talanta*, 2007, **72**, 546-553.